

Is the misalignment of the Local Group velocity and the 2MRS dipole typical in a Λ CDM & halo model?

Pirin Erdoğdu^{1,2} and Ofer Lahav¹

¹*Department of Physics and Astronomy, University College London, London, WC1E 6BT and*

²*Department of Science and Engineering, American University of Kuwait, P.O. Box 3323, Safat 13034, Kuwait*

(Dated: October 29, 2018)

We predict the acceleration of the Local Group generated by the 2MASS Redshift Survey (2MRS) within the framework of Λ CDM and the halo model of galaxies. We show that as the galaxy fluctuations derived from the halo model have more power on small scales compared with the mass fluctuations, the misalignment angle between the CMB velocity vector and the 2MRS dipole is in reasonable agreement with the observed 21° . This statistical analysis suggests that it is not necessary to invoke a hypothetical nearby galaxy or a distant cluster to explain this misalignment.

PACS numbers: 98.56

I. INTRODUCTION

In the late 1980s and early 1990s, the near alignment of the *IRAS* and the optical dipoles with the Local Group velocity relative to the cosmic microwave background (CMB, [1, 2, 3, 4, 5, 6, 7, 8]) were used to verify the gravitational instability picture of structure formation and the scale of convergence was used to assess the validity of the then popular Standard Cold Dark Matter (SCDM) model ([9] hereafter (LKH) and [10], hereafter JVV).

The distance at which most of the Local Group (LG) peculiar velocity is generated (*the convergence depth*) has remained a contentious issue for the past twenty five years. The observed misalignment between the vectors derived from the galaxy survey and the CMB has been attributed to several factors:

1. The linear perturbation theory of density fluctuations is correct only to first order density contrast, δ . There may be contributions to the LG dipole from small scales which would cause gravity and the velocity vectors to misalign.
2. The selection effects of the surveys from which these vectors are calculated will increase the shot noise-error especially at large distances causing misalignments.
3. There may be uncertainties in the assumptions in galaxy formation and clustering. For example, the mass-to-light ratios might differ according to type and/or vary with luminosity or the galaxy/cluster biasing might be non-linear and/or scale dependent.
4. There may be a significant contribution to the LG dipole from structure further away than the maximum distance of the surveys studied.
5. The direction of the LG dipole may be affected by nearby galaxies or distant clusters behind the *Zone of Avoidance* (ZoA), which are not sampled by most surveys.

The estimates of the convergence depth are highly sensitive to the type of data and the analysis performed. For

example, the convergence depth estimated from galaxy clusters consistently disagree with the estimates from galaxy surveys (e.g. see [11] and the references therein). Moreover, the treatment of the ZoA plays an important factor in dipole determinations. Exclusion of bright galaxies changes the dipole misalignment direction considerably (from 21° to 14° , [11]). These bright galaxies lie within the ZoA and are excluded from most dipole analyses. This also highlights the vital role non-linear dynamics introduced by nearby objects play in dipole considerations. The analysis of the convergence of the dipole is further complicated by the redshift distortions on small and large scales which introduce systematic errors [12].

Recently, the new dipole determinations from the 2MASS Redshift Survey (hereafter 2MRS, [11, 13, 14, 15]) brought up once again the question of alignment and convergence. For example, [16] attempted to fix the observed misalignment by placing a hypothetical object behind the ZoA and [17] tried to mitigate the non-linear and shot noise effects by removing nearby objects in order to increase the correlation between the dipole determined from the CMB and the 2MRS. Furthermore, two recent studies of the peculiar velocity surveys indicated a large convergence depth. [18] found a strong bulk flow on scales out to $300 h^{-1}\text{Mpc}$ using peculiar velocity data from an X-ray cluster sample. [19] reported a large-scale bulk flow beyond $50 h^{-1}\text{Mpc}$ from a comprehensive compilation of peculiar velocity data. Both these papers claimed that these convergence depths, determined by their studies, were difficult to explain within the framework of standard Λ CDM model of cosmology.

Here we take a different approach, updating the LKH and JVV calculations to include two major developments in cosmology: the Λ CDM concordance model (replacing the old SCDM and a halo model for the galaxy power spectrum (replacing the naive linear biasing model)). In the next section, we consider the expected misalignment between the peculiar velocity of the LG and the acceleration vector estimates. We expect that the Λ CDM model will give a poorer misalignment compared to the SCDM model since it has a larger coherence length. Adding the

halo model for galaxy biasing will further increase the power of density fluctuations on small scales and therefore the misalignment angle. In Section 3, we consider the convergence of the acceleration from the 2MRS survey. In Section 4, we show that the observed convergence is highly probable in our model. In the last section we discuss limitations of our calculations and future work.

II. ALIGNMENT

The most popular mechanism for the formation of large-scale structure and motions in the Universe is the gravitational growth of primordial density perturbations. According to this paradigm the peculiar acceleration vector $\mathbf{g}(\mathbf{r})$ induced by the matter distribution around position \mathbf{r} is related to the mass by

$$\mathbf{g}(\mathbf{r}) = G\bar{\rho} \int_{\mathbf{r}}^{\infty} d^3\mathbf{r}' \delta_m(\mathbf{r}') \frac{\mathbf{r}' - \mathbf{r}}{|\mathbf{r}' - \mathbf{r}|^3} \quad (1)$$

where $\bar{\rho}$ is the mean matter density and $\delta_m(\mathbf{r}) = (\rho_m(\mathbf{r}) - \bar{\rho})/\bar{\rho}$ is the density contrast of the mass perturbations. In linear theory, the peculiar velocity field, $\mathbf{v}(\mathbf{r})$, and the peculiar acceleration vector, $\mathbf{g}(\mathbf{r})$, should be parallel with a constant of proportionality.

For $\mathbf{v}(\mathbf{r})$, we use a value derived from the CMB dipole. Using the first year of data from WMAP, [20] and the revised values of the motion of the Sun relative to the LG a velocity derived by [21], we find a LG velocity relative to the CMB of $v_{LG} = 627 \pm 22 \text{ kmsec}^{-1}$, towards $(l_{LG} = 273^\circ \pm 3^\circ, b_{LG} = 29^\circ \pm 3^\circ)$. The LG dipole, $\mathbf{d}(\mathbf{r})$ (in kmsec^{-1}), used as a proxy for $\mathbf{g}(\mathbf{r})$, is estimated from a galaxy survey and can be written as a summation of all the galaxies in that survey (Equation 13 in [11]):

$$\mathbf{d}(\mathbf{r}) = \frac{H_0 \Omega_m^\gamma}{\rho_L b_L} \sum_i^N w_{L_i} S_i \hat{\mathbf{r}}_i, \quad (2)$$

where ρ_L is the luminosity density, b_L is the luminosity bias factor introduced to account for the dark matter haloes not fully represented by the galaxies (hereafter we assume $b_L = 1$). The index γ appears in the growth function $f = d \ln \delta / d \ln a \approx \Omega_m^\gamma$ [22] and is an important diagnostic for distinguishing between Λ CDM and alternative models of gravity. It has little dependence on the cosmological constant [23], and a slight dependence on the dark energy equation of state parameters w [24]. Recent refined calculations predict $\gamma = 0.55$ for the Λ CDM concordance model, and $\gamma = 0.69$ [25] for a particular modified gravity model, DGP braneworld gravity [26].

In equation 2, S_i is the flux of galaxy i and w_{L_i} is the luminosity weighting function written as:

$$w_{L_i} = \frac{1}{\int_{L_{\text{lim},i}}^{\infty} L \Phi(L) dL}, \quad (3)$$

where $\Phi(L)$ is the luminosity function and $L_{\text{lim},i}$ is the minimum luminosity at a distance r_i (see [11] for a full derivation). The Poisson shot noise of \mathbf{d} is estimated as

$$\sigma_{sn}^2 = (H_0 \Omega_m^\gamma)^2 \sum_i^N (w_{L_i} S_i \hat{\mathbf{r}}_i)^2. \quad (4)$$

For a whole sky survey, the non-zero elements of the covariance matrix are given as follows:

$$C_{dd} = \frac{1}{3} \langle \mathbf{d} \cdot \mathbf{d} \rangle = \frac{H_0^2 \Omega_m^{2\gamma}}{3(2\pi)^3} \int \widehat{W}_{\mathbf{d}}^2(k) P_{gg}(k) dk^3 \quad (5)$$

and

$$C_{vv} = \frac{1}{3} \langle \mathbf{v} \cdot \mathbf{v} \rangle = \frac{H_0^2 \Omega_m^{2\gamma}}{3(2\pi)^3} \int \widehat{W}_{\mathbf{v}}^2(k) P_{mm}(k) dk^3 \quad (6)$$

and

$$C_{dv} = \frac{1}{3} \langle \mathbf{d} \cdot \mathbf{v} \rangle = \frac{H_0^2 \Omega_m^{2\gamma}}{3(2\pi)^3} \int \widehat{W}_{\mathbf{v}}(k) \widehat{W}_{\mathbf{d}}(k) P_{gm}(k) dk^3, \quad (7)$$

where P_{gg} and P_{mm} denote the galaxy and the dark matter power spectrum, respectively and P_{gm} denotes the galaxy-dark matter cross spectrum.

The expected misalignment angle between \mathbf{v} and \mathbf{d} is (JVW and LKH):

$$p(\theta|\mathbf{v}) = \sin(\theta) \exp(-1/(2\theta_*^2)) \left\{ \frac{y}{\sqrt{2\pi}} + \left(\frac{1+y^2}{2} \right) \exp(y^2/2) \left[1 + \text{erf}(y/\sqrt{2}) \right] \right\}, \quad (8)$$

where θ is the angle between the two vectors, $\theta_* \equiv [\sqrt{1-c^2}/c]/(\mathbf{v}/C_{vv}^{1/2})$ (in radians) and $c \equiv [C_{dv}^2/(C_{vv}C_{dd})]^{1/2}$ and $y \equiv \cos(\theta)/\theta_*$. In the case where θ_* is small, the probability distribution $p(\cos(\theta)|\mathbf{v})$ tends to bi-variate Gaussian and θ_* measures the expected scatter.

A. Window Functions

We assume the LG is a sphere with radius $r_{LG} = 1.6h^{-1} \text{ Mpc}$ and the LG velocity is produced by the matter distribution out to horizon. In Fourier space, the window function of the velocity vector \mathbf{v} , determined from the CMB dipole, varies as $1/k$:

$$\widehat{W}_{\mathbf{v}}(k) = \frac{j_0(kr_{LG})}{k}. \quad (9)$$

For the flux-weighted dipole $\widehat{W}_{\mathbf{d}}(k)$ can be written as:

$$\begin{aligned} \widehat{W}_{\mathbf{d}}(k) &= 4\pi \int_{r_{LG}}^{r_{\text{max}}} r^2 dr W_{\mathbf{d}}(r) j_1(kr) \\ &= \frac{j_0(kr_{LG})}{k} - \frac{j_0(kr_{\text{max}})}{k}, \end{aligned} \quad (10)$$

where $W_{\mathbf{d}}(r) = \frac{1}{4\pi r^2}$ and r_{\max} is the maximum radius of the survey which we adopt as $r_{\max} = 130h^{-1}$ Mpc. We want to compare our findings with the observed 2MRS values and beyond this distance the shot-noise effects in the 2MRS becomes too large.

B. Calculating the Power Spectra

The *halo model* for non-linear clustering gained popularity during the past few years [27, 28, 29]. This model assumes that most matter in the Universe is structured as virialised halos and correlation function on large scales depends on the clustering of these halos whereas non-linear clustering of objects are related to the internal structure of the individual halos. This implies that the non-linear power spectrum $P_{nl}(k)$ can be divided into a quasi-linear, *inter halo* term $P_{2h}(k)$ and a non-linear *intra halo* term $P_{1h}(k)$:

$$P_{nl}(k) = P_{2h}(k) + P_{1h}(k). \quad (11)$$

C. The Dark Matter Power Spectrum

Within the halo model framework, the dark matter power spectrum can be written as (e.g. [30]),

$$P_{\text{dm}}^{(1h)}(k) = \int dM n(M) \left(\frac{M}{\bar{\rho}}\right)^2 |\hat{u}(k|M)|^2, \quad (12)$$

and

$$P_{\text{dm}}^{(2h)}(k) = P_{\text{dm}}^{\text{lin}}(k) \left[\int dM n(M) b(M) \left(\frac{M}{\bar{\rho}}\right) \hat{u}(k|M) \right]^2, \quad (13)$$

where the integrals are over the halo mass, M and $\bar{\rho}$ is the background density of the universe. We use transfer functions of [31] to calculate $P_{\text{dm}}^{\text{lin}}(k)$. In the expressions above, $n(M)$ is the halo mass function describes the number density of haloes of mass M , $b(M)$ is the halo bias factor and $\hat{u}(k|M)$ is the Fourier transform of the halo profile, $\rho(r)$.

For $n(M)$ and $b(M)$, we assume the forms proposed by [32]:

$$n(M)dM = \frac{\bar{\rho}}{M} f(\nu) d\nu, \quad (14)$$

$$\nu f(\nu) = A_* (1 + (q\nu)^{-p}) \left(\frac{q\nu}{2\pi}\right)^{1/2} e^{-q\nu/2}, \quad (15)$$

where $q = 0.707$, $p = 0.3$, and the normalisation $A_* \approx 0.3222$. The mass variable is defined as $\nu \equiv (\delta_{\text{sc}}(z)/\sigma(M))^2$, where $\delta_{\text{sc}}(z)$ is the linear-theory prediction for the present day overdensity of a region undergoing spherical collapse at redshift z ($\delta_{\text{sc}}(0) \approx 1.68$) and $\sigma(M)$ is the r.m.s. variance of the present day linear

power spectrum in a spherical top-hat which contains an average mass M .

The degree of bias is also a function of the halo mass:

$$b(M) = 1 + \frac{q\nu - 1}{\delta_{\text{sc}}(z)} + \frac{2p/\delta_{\text{sc}}(z)}{1 + (q\nu)^p}. \quad (16)$$

We also use the [33] dark matter halo density profile.

$$\rho(r) = \frac{\rho_s}{(r/r_s)(1 + r/r_s)^2} \quad (r < r_{\text{vir}}) \quad (17)$$

where r_s is the characteristic scale radius and ρ_s provides the normalization. The profile is truncated at the virial radius r_{vir} , which is obtained from the halo mass. We parametrize the profile in terms of the *concentration parameter* $c = r_{\text{vir}}/r_s$. The normalization for the mass M is

$$M = \int_0^{r_{\text{vir}}} \rho(r) 4\pi r^2 dr = 4\pi \rho_s r_s^3 \left[\ln(1 + c) - \frac{c}{1 + c} \right] \quad (18)$$

We assume that the concentration parameter c depends on halo mass M and redshift in a manner calibrated by numerical simulations ([34, 35]):

$$c(M, z = 0) = 11 \left(\frac{M}{M_0}\right)^{-0.13}, \quad (19)$$

where M_0 is obtained from equation by setting the variance of the linear power spectrum $\sigma(M_0, 0) = \delta_{\text{sc}} = 1.68$. For our adopted cosmological model we obtain $M_0 = 10^{12.13} h^{-1} M_{\odot}$.

D. The Galaxy Power Spectrum

The components of the galaxy power spectrum are similar to the dark matter power spectrum given above

$$P_{\text{gal}}^{(1h)}(k) = \int dM n(M) \frac{\langle N(N-1)|M \rangle}{\bar{n}_{\text{gal}}^2} |\hat{u}(k|M)|^2, \quad (20)$$

and

$$P_{\text{gal}}^{(2h)}(k) = P_{\text{dm}}^{\text{lin}}(k) \left[\int dM n(M) b(M) \frac{\langle N|M \rangle}{\bar{n}_{\text{gal}}} \hat{u}(k|M) \right]^2, \quad (21)$$

Here, $\langle N|M \rangle$ and $\langle N(N-1)|M \rangle$ are the first and second factorial moments of the halo occupation distribution, $P(N|M)$, respectively, \bar{n}_{gal} is the average number density of galaxies. The halo occupation distribution (HOD) is a parametrized description of how galaxies populate dark matter haloes as a function of the halo mass M . We adopt simple models motivated by results from simulations and semi-analytic calculations (e.g. [36])

$$\langle N|M \rangle = \begin{cases} (M/M_0)^{\beta} & (M \geq M_{\text{cut}}) \\ 0 & (M < M_{\text{cut}}) \end{cases} \quad (22)$$

where M_0 and β are free parameters and M_{cut} is determined by matching \bar{n}_{gal} to the value derived from the 2MRS ($\bar{n}_{\text{gal}} = 7.7 \times 10^{-4} h^3 \text{Mpc}^{-3}$). The second moment of $P(N|M)$ is:

$$\langle N(N-1)|M \rangle = \begin{cases} \langle N|M \rangle^2 & (M \geq 10^{13} h^{-1} \text{M}_\odot) \\ (\alpha \langle N|M \rangle)^2 & \text{otherwise,} \end{cases} \quad (23)$$

where $\alpha = \log \sqrt{M/h^{-1} 10^{11} \text{M}_\odot}$.

For our halo model parameters, we use $M_0 = 10^{14.16} h^{-1} \text{M}_\odot$ and $\beta = 0.85$, derived for 2MASS galaxies (see Table 1 of [37]). These values are quite typical for red galaxies and varying the parameters slightly does not affect the results.

We note that on large scales the galaxy power spectrum takes the simple form:

$$P_{\text{gal}}(k) = b^2 P_{\text{dm}}^{\text{lin}}(k) + 1/\bar{n}_{\text{gal}} \quad (24)$$

The last term is the shot noise term, which we found to give the very r.m.s. contribution to the shot-noise in the dipole as the empirical estimate (Equation 4).

E. The Galaxy-Dark Matter Cross Power Spectrum

Using the expressions above, the galaxy dark matter cross power spectrum components can be written as

$$P_{\text{gm}}^{(1h)}(k) = \int dM n(M) \frac{M}{\bar{\rho}} \frac{\langle N|M \rangle}{\bar{n}_{\text{gal}}} |\hat{u}(k|M)|^2, \quad (25)$$

and

$$P_{\text{gm}}^{(2h)}(k) = P_{\text{dm}}^{\text{lin}}(k) \left[\int dM n(M) b(M) \frac{\langle N|M \rangle}{\bar{n}_{\text{gal}}} \hat{u}(k|M) \right] \times \left[\int dM n(M) b(M) \left(\frac{M}{\bar{\rho}} \right) \hat{u}(k|M) \right]. \quad (26)$$

III. CONVERGENCE

We now turn to the question of the convergence of the acceleration vector derived from a galaxy survey given the velocity of the CMB. We recalculate the conditional probability, $p(\mathbf{d}|\mathbf{v})$ given in equation 8 within a series of successively larger concentric spheres centred on the LG. In this case, the value of the covariance matrix element C_{vv} remains the same and we recalculate C_{dv} and C_{dd} using a series of window functions:

$$\widehat{W}_{\mathbf{d}}(k) = \frac{j_0(kr_{\text{LG}})}{k} - \frac{j_0(kR)}{k}. \quad (27)$$

where R is the outer limit of each shell.

The expected dipole velocity given the CMB dipole is then written as:

$$\mathbf{d}(R) = \frac{C_{\text{dv}}(R)}{C_{\text{vv}}} \mathbf{v}_{\text{CMB}} \quad (28)$$

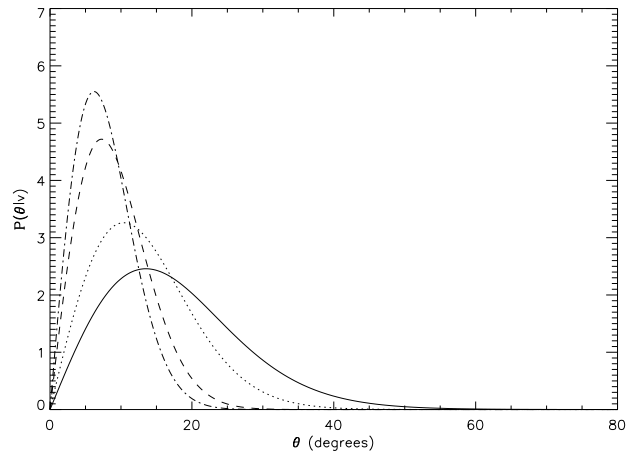


FIG. 1: The probability distribution functions for misalignment angle Θ between the galaxy survey dipole and the CMB velocity vectors. The dashed-dotted line denotes the misalignment angle calculated using $P(k)_{\text{mm}}^{\text{lin}}$ only for SCDM model ((1) in Table 1), the dashed line is calculated using Λ CDM and $P(k)_{\text{mm}}^{\text{nl}}$ ((3) in Table 1). The solid line is calculated using Equations 5, 6 and 7 ((4) in Table 1). The dotted line is the same as the solid line but using $P(k)_{\text{gg}} = P(k)_{\text{gg}}^{2h}$ ((5) in Table 1).

and the ‘1 sigma’ scatter in the velocity is $|\mathbf{d}(R)| \pm \sqrt{3\sigma^2}$ with $\sigma^2 = C_{\text{dd}}(R) \left(1 - \frac{C_{\text{dv}}(R)^2}{C_{\text{dd}}(R)C_{\text{vv}}}\right)$.

IV. RESULTS

In Figure 1, we plot a family of $p(\theta|\mathbf{v})$ curves given by equation 8. The dashed-dotted line is calculated using the old SCDM model with $\Omega_m = 1.0$, $\sigma_8 = 0.6$, the Hubble constant $H_0 = 50 \text{kmsec}^{-1} \text{Mpc}^{-1}$ and the spectral index $n = 1$. For all other power spectra, we use WMAP5 fiducial parameters $\Omega_m = 0.26$, $f_b = 0.17$, $\sigma_8 = 0.79$, $H_0 = 72 \text{kmsec}^{-1} \text{Mpc}^{-1}$ and $n = 1$ [38].

We first consider the standard linear and non-linear Λ CDM dark matter power spectrum models with a linear biasing model of $b = 1$. We obtain almost identical curves (dashed line) with a scatter of $\theta_* = 7^\circ$. Both curves peak at around 8° . Changing the radius of the LG to $r_{\text{LG}} = 5h^{-1} \text{Mpc}$ has also a very small effect on the results. The narrowest scatter in the probability curve and the smallest expected misalignment angle is obtained using the SCDM model ($\theta_* = 6^\circ$, dashed-dotted line). This is expected since SCDM has a smaller coherence length than the Λ CDM model.

We then calculate the power spectra using the halo model for galaxies as well as for dark matter. The power spectrum shown by the black solid line includes both 1-halo and the 2-halo terms. The scatter for this model is the largest $\theta_* = 14^\circ$ and the probability curve peaks at the largest misalignment angle of the plotted curves (13.5°). In the galaxy halo model, the galaxies are more

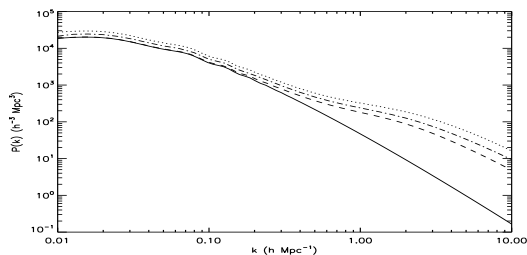


FIG. 2: The linear dark matter (P_{lin} , solid line), halo model dark matter (P_{dm} , dashed line), galaxy-dark matter (P_{gm} , dashed-dotted line) and galaxy-galaxy (P_{gal} , dotted line) power spectra. The power spectra are normalized to be equal on very large scales (very small k).

clustered than the dark matter (see Figure 2) and thus the covariance matrix elements are much larger than the ones we obtain with the linear bias models. The halo model is used to describe all haloes within a survey. Thus the 2-halo term represents the clustering of all haloes on large scales and the 1-halo term is related to the internal clustering of each halo in the survey. We also want to model the dipole induced by clusters of galaxies rather than galaxies themselves. For this, we plot the probability function calculated using 2-halo term only ($P_{gg}(k) = P_{2h}(k)$, the dotted line) which peaks around 10° and gives $\theta_* = 11^\circ$. When we add the 1-halo term (solid line), we are adding the galaxy component to our model. This increases the shot-noise which causes the CMB and the galaxy survey dipoles to decorrelate as confirmed by our value for θ_* . Changing the radius of the LG to $r_{\text{LG}} = 5h^{-1}$ Mpc mitigates the non-linear effects, reducing the scatter, $\theta_* = 10^\circ$.

We also calculate the r.m.s. velocity of our LG models, $\langle v_{\text{LG}}^2 \rangle^{1/2} = (3C_{vv})^{1/2}$. For our Λ CDM cosmology with $\sigma_8 = 0.79$, we obtain 412 and 430 kmsec^{-1} for the linear and non-linear power spectra, respectively. We note the observed LG velocity amplitude, 621 kmsec^{-1} , is larger than these r.m.s. values.

We summarize the results presented in Figure 1 in Table 1. We present the probability obtaining the actual observed angle (21°) and the integrated probability for θ to lie below the observed value which provides a frequentist test. The two columns indicate that the observed dipole is highly unlikely in both the linear and non-linear models which do not include a non-linear bias model for galaxies. Neither are we able to approximate the observed value without including the 1-halo term to the galaxy power spectrum. But, using the halo model for both galaxies and the dark matter, results in a mean close to that of 21° .

In Figure 3, we plot the expected dipole velocity given the CMB dipole (Equation 28, solid line) and its scatter (dashed line). In the top panel, we use only the linear power spectrum (the first model in Table 1) and the bottom panel is the velocity convergence with the full halo model treatment (the fourth model in Table 1). The

plots in the left panel are the predicted amplitudes of the acceleration on the LG as a function of distance. The right plots show the convergence of the angle between the galaxy survey dipole and the CMB dipole. We also plot the observed values of the acceleration amplitude and the misalignment angle from the 2MRS survey obtained using the flux-weighted selection function ([11]) as an illustrative example. There are many determinations of the dipole misalignment angle from the 2MRS data ranging from 14° [11] to 50° [14] depending on the type of analysis performed. The near-infrared flux weighted dipoles are more robust than the number weighted schemes because they closely approximate a mass-weighted dipole, bypassing the effects of redshift distortions and require no preferred reference frame. Our analysis holds for either scheme or the choice of reconstruction technique since we account for the correct data vector for selection effects and compare like with like.

The 2MRS acceleration grows rapidly out to $\approx 50h^{-1}$ Mpc after that it flattens off. The misalignment angle drops to 12° at $\approx 50h^{-1}$ Mpc but then increases at larger distances. This behaviour is not seen for either of the models. This is not unexpected, however, since the increase in amplitude at $\approx 50h^{-1}$ Mpc and then its consequent decrease at $\approx 60h^{-1}$ Mpc is attributed to the tug-of-war between the Great Attractor and the Pisces-Perseus Supercluster which are not accounted in the statistical (r.m.s.) models.

In theory, one can equate the velocity inferred from the CMB measurements with the value derived from a galaxy survey and obtain a value for Ω_m . In practice, however, the galaxy surveys do not measure the true total velocity due their finite depth and the predicted amplitude of the reconstructed velocity depends the combination of matter density and the biasing parameter b which is usually not known to great accuracy. However, one would expect Ω_m and b inferred from the LG velocity to have observationally viable values. Figure 3 shows that the amplitudes for both of the models are similar to observations, but the non-linear model has higher amplitude due to higher small-scale power and is closer to the observed values. In both models, more than half of the predicted LG velocity signal is generated within $\approx 30h^{-1}$ Mpc. The non-linear galaxy model decorrelates the angles and incorporates shot-noise effects and closely resembles the observed convergence.

V. DISCUSSION

We have compared estimates for of the acceleration as derived from a 2MRS like survey and the motion of the LG in a Λ CDM universe both within and without the halo model framework. We showed that a combination of linear theory with the halo model predicts convergence and misalignment very much in agreement with the observed 2MRS dipole.

We should note our analysis assumes linear perturba-

TABLE I: Dipoles constrained by the velocity of the local group, the characteristic misalignment angle θ_* is given in degrees. The observed misalignment angle $\theta_{obs} = 21^\circ$ is calculated from the 2MRS survey (Erdoğdu et al. 2006b). The assumed cosmological parameters $(\sigma_8, h_0, \Omega_m, f_b)$ are (0.79, 0.72, 0.26, 0.17) for Λ CDM and (0.6, 0.5, 1.0, 0.044) for SCDM.

Model	θ_* (deg)	$P(\theta_{obs})/\max(P(\theta \mathbf{v}))$	Percent below θ_{obs}
(1) SCDM, $P_{dm}^{lin}(k)$	6.3	0.02	99.6
(2) Λ CDM, $P_{dm}^{lin}(k)$	7.2	0.08	98.1
(3) Λ CDM, $P_{dm}^{nl}(k)$	7.2	0.08	98.1
(4) Λ CDM, Halo model for Galaxies	13.5	0.78	67.2
(5) Λ CDM, $P_{gg}(k) = P_{gg}^{2h}(k)$	10.4	0.45	85.3

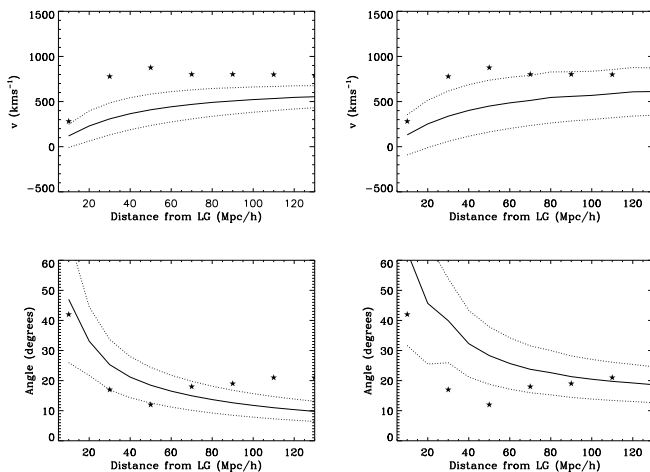


FIG. 3: **Top Panel:** The predicted LG velocity within a series of successively larger concentric spheres centred on the LG given by Equation 28 and the 1-sigma scatter. **Bottom Panel:** The misalignment angle as a function of distance. **Left:** The convergence is calculated using linear dark matter power spectrum only ((2) in Table 1). **Right:** The convergence is calculated using non-linear galaxy power spectrum and galaxy-dark matter cross spectrum (Case (4) in Table 4).

tion theory but we are using a non-linear galaxy power spectrum, so our treatment is incomplete. A more consistent way would be to use N-body simulations (e.g. [39]) and semi-analytic models galaxy formation but this is beyond the scope of the work presented in this paper. Here, we tested if a non-linear power spectrum model with a more sophisticated biasing formula could predict the observed acceleration better than a linear power spectrum. Indeed, our results indicate the flow in our location in the universe is quite typical for a Λ CDM model. A non-linear velocity-acceleration relation will increase the misalignment angle [40]. Recently, Lavaux et al. [14] used the

2MRS reconstructed peculiar velocity field to estimate a LG velocity misalignment of $\approx 50^\circ \pm 22^\circ$ (at 95% confidence). They suggest the dipole directions should agree to within 25° at 95% confidence. From Figure 3 (right panel), the expected misalignment angle is $\approx 29^\circ \pm 7^\circ$ at $130 h^{-1}$ Mpc. Our analysis should be viewed as a conservative estimate of the expected misalignment error. Thus, even a dipole misalignment is as high as reported by [14] is reconcilable with a Λ CDM model given their estimated error.

We would like to emphasize that we have assumed that the accelerations are estimated from a whole sky survey. It is possible to incorporate the effect of ZoA (see Appendix of LKH) which would increase the scatter substantially. We note that we are able to reproduce the observed values very well without modeling missing structures in the masked regions as suggested by [16]. We further note that many dedicated searches of the ZoA did not detect such massive structures (see e.g. [41, 42, 43, 44, 45, 46, 47, 48, 49, 50, 51]). Our analysis should be understood in the r.m.s. sense. It does not pick out directions. As noted by others (e.g. [16]), most of the LG misalignment lies along the direction of the galactic centre, the region of most obscuration, and this is another route for exploring the misalignment.

To summarize, we presented a fresh analysis of the fundamental problem of the origin of motion on the Local Group. We conclude that the newly observed 2MRS dipole is in accord with what we would expect in a Λ CDM universe within the context of the halo model.

VI. ACKNOWLEDGEMENTS

We thank Michal Chodorowski, Gert Hutsi and Renée Kraan-Korteweg for helpful discussions. PE would like to thank UCL for its hospitality. OL acknowledges the support of a Wolfson Royal Society Research Merit Award.

[1] Yahil A., Walker D. & Rowan-Robinson M., 1986, ApJ, 301, L1

[2] Meiksin A. & Davis M., 1986, AJ, 91, 191

- [3] Harmon R.T., Lahav O. & Meurs E.J.A., 1987, MNRAS, 228, 5
- [4] Villumsen J.V. & Strauss M.A., 1987, ApJ, 322, 37
- [5] Lahav O., Rowan-Robinson M. & Lynden-Bell, 1988, MNRAS, 234, 677
- [6] Lynden-Bell D., Lahav O. & Burstein D., 1989, MNRAS, 241,325
- [7] Strauss M. A., Yahil A., Davis M., Huchra J. P., Fisher K., ApJ, 1992, 397, 395
- [8] Webster M., Lahav O. & Fisher K., 1997, MNRAS, 287,425
- [9] Lahav O., Kaiser N., Hoffman Y., 1990, ApJ, 352, 448
- [10] Juskiewicz R., Vittorio N., Wyse R., 1990, ApJ, 352, 408
- [11] Erdođdu P., et al., 2006a, MNRAS, 368, 1515
- [12] Kaiser N., 1987, MNRAS, 227, 1
- [13] Erdođdu P., et al., 2006b, MNRAS, 373, 45
- [14] Lavaux G., Tully R. B., Mohayaee R., Colombi, S., 2008, arXiv:astro-ph/0810.3658v2
- [15] Crook A., Silvestri A., Zukin P., 2009, arXiv:astro-ph/0906.2411
- [16] Loeb A., Narayan R., 2008, MNRAS, 386, 2221
- [17] Chodorowski M. J., Coiffard J., Bilicki M., Colombi S., Cielciag P., 2008, astro-ph/0706.0619
- [18] Kashlinsky A., Atrio-Barandela F., Kocevski D., Ebeling H., 2008, ApJ, 686, 49
- [19] Watkins R., Feldman H. A., Hudson M. J., 2009, MNRAS, 392, 743
- [20] Bennett C.L., et al. , 2003, ApJS, 148, 1
- [21] Courteau S. & Van Den Bergh S., 1999, AJ, 118, 337
- [22] Peebles P. J. E., *The Large-Scale Structure of the Universe*, Princeton: Princeton Univ. Press, Princeton, N.J., USA
- [23] Lahav O., Lilje P. B., Primack J. R., Rees M. J., 1991, MNRAS, 251, 128
- [24] Wang L., Steinhardt P. J., 1998, ApJ, 508, 483
- [25] Linder E. V., Cahn R. N., 2007, APh, 28, 481
- [26] Dvali G., Gabadadze G., Porrati M., 2000, PhLB, 485, 208
- [27] Ma C., Fry J. N., 2000, ApJ, 543, 503
- [28] Peacock J.A., Smith R.E., 2000, MNRAS, 318, 1144
- [29] Seljak U., 2000, MNRAS, 318, 203
- [30] Cooray A., Sheth R. K., 2002, Phys. Rep., 371, 1
- [31] Eisenstein D. J., Hu W., 1998, ApJ, 496, 605
- [32] Sheth R. K., Tormen G., 1999, MNRAS, 308, 119
- [33] Navarro J. F., Frenk C. S., White S. D. M., 1997, ApJ, 490, 493
- [34] Bullock J. S., Kolatt T. S., Sigad Y., Somerville R. S., Kravtsov A. V., Klypin A. A., Primack J. R., Dekel A., 2001, MNRAS, 321, 559
- [35] Zehavi I. et al., 2004, ApJ, 608, 16
- [36] Kravtsov A. V., Berlind A. A., Wechsler R. H., Klypin A. A., Gottlöber S., Allgood B., Primack J. R., 2004, ApJ, 609, 35
- [37] Lin Y., Mohr J.J., Stanford S.A., 2004, ApJ, 610, 745
- [38] Dunkley J. et al. 2009, ApJ Supp., 180, 306
- [39] Davis M., Strauss M.A., Yahil A., 1990, ApJ, 372, 394
- [40] Davis M., Nusser A., Willick J., 1996, ApJ, 473, 22
- [41] Ebeling, H., Mullis, C. R., Tully, R. B. 2002, ApJ, 580, 774
- [42] Ebeling H., Kocevski D., Tully R. B., Mullis C. R. 2005, *Nearby Large-Scale Structures and the ZoA*, 329, 83
- [43] Kocevski, D. D., Ebeling, H., Mullis, C. R., Tully, R. B. 2005, *ArXiv Astrophysics e-prints*, arXiv:astro-ph/0512321
- [44] Kocevski D. D., Ebeling H., 2006, ApJ, 645, 1043
- [45] Roman, A. T., Takeuchi, T. T., Nakanishi, K., Saito, M. 1998, PASJ, 50, 47
- [46] Wakamatsu K., Malkan, M. A., Nishida M. T., Parker Q. A., Saunders W., Watson F. G. 2005, *Nearby Large-Scale Structures and the ZoA*, 329, 189
- [47] Hasegawa T., et al. 2000, MNRAS, 316, 326
- [48] Meyer M. J., et al. 2004, MNRAS, 350, 1195
- [49] Henning P. A., Kraan-Korteweg R. C., Staveley-Smith L. 2005, *Nearby Large-Scale Structures and the ZoA*, 329, 199
- [50] Kraan-Korteweg R. C., Lahav 2000 *A&A Rev*, 10, 211
- [51] Kraan-Korteweg R. C., Shafi N., Koribalski B., Staveley-Smith L., Buckland P., Henning, P. A., Fairall, A. P. 2007, arXiv:0710.1795